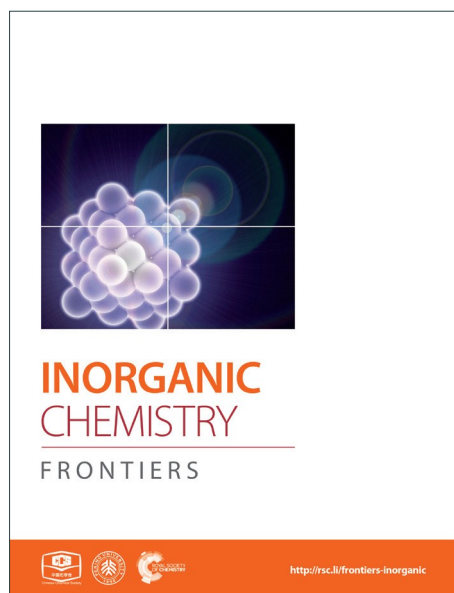
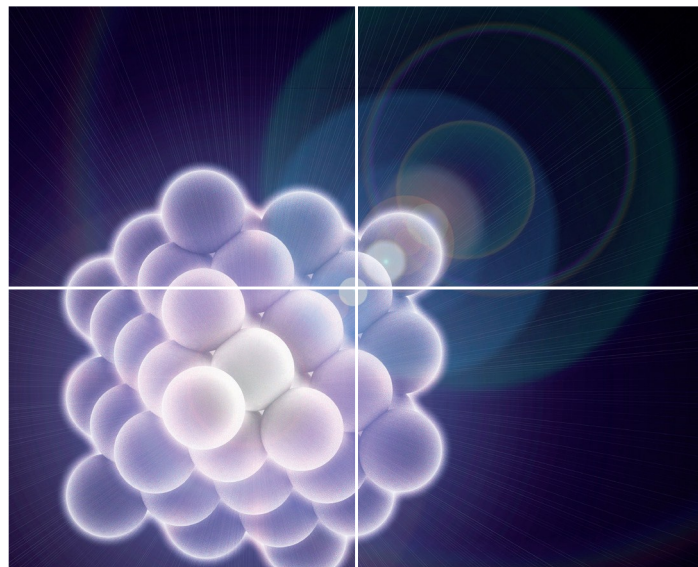


INORGANIC CHEMISTRY

FRONTIERS

Accepted Manuscript



This is an *Accepted Manuscript*, which has been through the Royal Society of Chemistry peer review process and has been accepted for publication.

Accepted Manuscripts are published online shortly after acceptance, before technical editing, formatting and proof reading. Using this free service, authors can make their results available to the community, in citable form, before we publish the edited article. We will replace this *Accepted Manuscript* with the edited and formatted *Advance Article* as soon as it is available.

You can find more information about *Accepted Manuscripts* in the [Information for Authors](#).

Please note that technical editing may introduce minor changes to the text and/or graphics, which may alter content. The journal's standard [Terms & Conditions](#) and the [Ethical guidelines](#) still apply. In no event shall the Royal Society of Chemistry be held responsible for any errors or omissions in this *Accepted Manuscript* or any consequences arising from the use of any information it contains.



Journal Name

ARTICLE

Metal-Organic Aerogels Based on Dinuclear Rhodium Paddle-Wheel Units: Design, Synthesis and Catalysis

Baofu Zhu,^a Gang Liu,^a Lianfen Chen,^a Liqin Qiu,^a Liuping Chen,^a Jianyong Zhang,^a Li Zhang,^{*a} Mihail Barboiu,^{ab} Rui Si,^d and Cheng-Yong Su^{*ac}

Received 00th January 20xx,
Accepted 00th January 20xx

DOI: 10.1039/x0xx00000x

www.rsc.org/

A series of metal-organic gels (MOG-Rh-**1a-d**) are synthesized by the reaction of dirhodium(II) tetraacetate (Rh₂(OAc)₄) and the tricarboxylic acid 4,4',4''-[1,3,5-benzenetriyltris(carbonylimino)]tristribenzoic acid (H₃btctb) in DMF/water or DMF/methanol. After drying with subcritical carbon dioxide, the metal-organic aerogels (MOA-Rh-**1a-d**) were obtained and fully characterized by EA, SEM, TEM, TGA, PXRD, UV-vis, XPS and EXAFS measurements. The presence of dinuclear rhodium paddle-wheel units and the Rh²⁺ valence in the aerogels are proven by UV-vis, XAS and XPS spectra. As revealed by the SEM and TEM images, the aerogels have a general porous structure with entangled worm-like morphology. The porosity of the aerogels is confirmed by nitrogen adsorption at 77K, and the sorption isotherms present type-IV curves, indicating that both micro- and meso-porosity are present. The accessibility of the mesopores is verified by dye uptake such as methylene blue (MB, 14.4 × 6.1 Å²) and Coomassie brilliant blue R-250 (BBR-250, 22 × 18 Å²). The catalytic tests disclose that MOA-Rh-**1d** is effective in coupling reaction of CO₂ and epoxides as well as intramolecular C-H amination of viny azides. MOA-Rh-**1d** can be recycled easily and used for at least ten runs with the yields in the range of 91-98% in CO₂ conversion reactions.

1. Introduction

As a kind of new emerging metal-organic materials (MOMs), metal-organic gels (MOGs) have attracted significant research interests during the last 15 years, due to their applications in gas/dye adsorption, catalysis, sensing, optics, magnetic materials, etc.¹⁻⁵ The gelling agents in MOGs are often discrete metal coordination complexes or short-range ordered coordination polymers, which enable the formation of extended networks through coordination and other weak interactions. Most of the reported MOGs are constructed from single metal ions, among which, Fe²⁺, Co²⁺, Cu²⁺, Ag⁺, Au⁺, Pd²⁺ and Pt²⁺ are often used. In a few Au and Pt-containing MOGs, Au⁺...Au⁺ (d¹⁰-d¹⁰) or Pt²⁺...Pt²⁺ (d⁸-d⁸) interactions may exist and help the MOGs exhibit interesting luminescence properties.^{6,7} Nevertheless the constructions of MOGs with strong metal-metal bonds have been never explored.

Paddle-wheel complexes are characterized as two metal centers bridged by four ligands. Depending on the metal centers used, direct metal-metal bonding (e.g. Mo²⁺-Mo²⁺ quadruple bond in Mo₂⁴⁺, Ru²⁺-Ru³⁺ bond with a bond order of 2.5 in Ru₂⁵⁺ and Rh²⁺-Rh²⁺ single bond in Rh₂⁴⁺) can occur. The dinuclear paddle-wheel unit has emerged as a common four-connected building block in the synthesis of other kinds of MOMs, metal-organic cages (MOCs) and metal-organic frameworks (MOFs). Cotton and Murillo have employed bimetallic units, especially Mo₂⁴⁺, Ru₂⁵⁺ and Rh₂⁴⁺, in the construction of polygons such as molecular loops, triangles and squares, polyhedra such as tetrahedron and octahedron, and coordination polymers.⁸⁻¹¹ Zhou et al. developed a series of MOCs derived from dimetal paddlewheel units (e.g. Mo₂⁴⁺ and Ru₂⁴⁺ bimetallic units) and diprotic carboxylate ligands.^{12,13} Mori et al. developed a series of dimolybdenum, diruthenium and dirhodium-containing MOFs employing either dicarboxylic acids or metalloporphyrin as ligands.¹⁴⁻¹⁶ Dincă group has synthesized the MOF of Ru₃(btc)₂ (btc³⁻ = benzene-1,3,5-tricarboxylate), which has the similar structure as HKUST-1 (Cu₃(btc)₂), using Ru₂Cl(OPiv)₄ (OPiv = ^tBuCO₂⁻) as the ruthenium source.¹⁷ Kaskel et al. have developed a MOF with dirhodium units synthesized from Rh₂(OAc)₄ and H₃btc.¹⁸ Our group has prepared a lantern-type MOC consisting of two dirhodium units joined by four dicarboxylic acids.¹⁹

Dirhodium complexes are taking on an increasingly important role in catalyzing a variety of organic reactions in which novel C-C, C-N and C-O bond formation reactions are involved, giving rise to many interesting as well as important organic compounds.²⁰ A limited number of catalytic MOCs and

^a MOE Laboratory of Bioinorganic and Synthetic Chemistry, Lehn Institute of Functional Materials, School of Chemistry and Chemical Engineering, Sun Yat-Sen University, Guangzhou 510275, China. E-mail: zhli99@mail.sysu.edu.cn; cecscy@mail.sysu.edu.cn

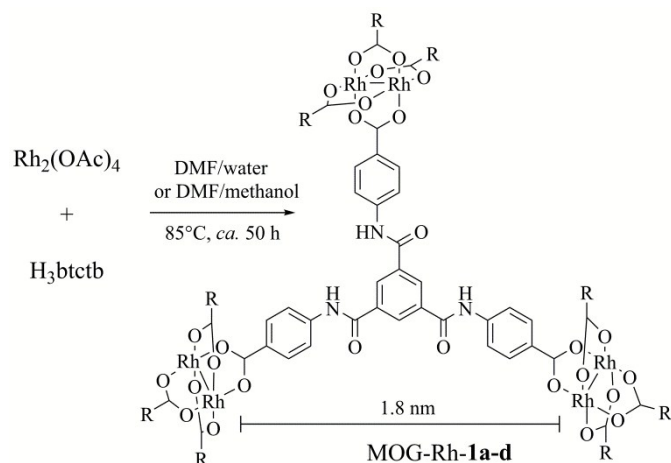
^b Institut Européen des Membranes—University of Montpellier, ENSCM/UMR CNRS 5635, Place Eugène Bataillon, CC 047, F-34095 Montpellier, France

^c State Key Laboratory of Organometallic Chemistry, Shanghai Institute of Organic Chemistry, Chinese Academy of Sciences, Shanghai 200032, China

^d Shanghai Institute of Applied Physics, Chinese Academy Sciences, Shanghai Synchrotron Radiation Facility, Shanghai 201204, China

[†] Electronic Supplementary Information (ESI) available: [Gelation study, the stability tests of the wet gels, the characterizations (e.g. EDS, TGA, PXRD, XPS UV-vis and EXAFS) of the aerogels, and heterogeneous catalysis]. See DOI: 10.1039/x0xx00000x

MOFs with dinuclear rhodium units have been synthesized, and their activities have been tested in organic reactions such as hydrogenation,^{16,18} cyclopropanation¹⁰ and C-H amination.¹⁹ Herein, the gels of MOG-Rh-**1a-d** have been prepared from the reaction of $\text{Rh}_2(\text{OAc})_4$ and 4,4',4''-[1,3,5-benzenetriyltris(carbonylimino)]tristribenzoic acid (H_3btctb) (Scheme 1), whose structures are based on dinuclear rhodium(II) paddlewheel units. To the best of our knowledge, this is the first report of MOGs based on Rh^{2+} - Rh^{2+} bonds.



Scheme 1. MOG Synthesis.

2. Experimental section

All the reagents in the present work were obtained from the commercial sources and used directly without further purification. The ligands 4,4',4''-[1,3,5-benzenetriyltris(carbonylimino)]tristribenzoic acid (H_3btctb), 1,3,5-tri(4-carboxyphenoxy)benzene (H_3tcpb) and 4,4',4''-[benzene-1,3,5-triyltris(azanediyl)]tribenzoic acid (H_3tatab) were synthesized according to the literature.²¹⁻²³ Vinyl azides are prepared following the reported procedures.²⁴

Cautions! Although we have not experienced any problem in the handling of the azides, extreme care should be taken when manipulating them due to their explosive nature.

2.1 Preparation of Gels and Aerogels

Typical procedure: A mixture of $\text{Rh}_2(\text{OAc})_4$ (10.0 mg, 0.0225 mmol) and H_3btctb (17.0 mg, 0.030 mmol) was dissolved in DMF (1 mL) with sonication, and then methanol (1 mL) was added to the reaction mixture. The resultant homogeneous solution was then left to stand at 85°C for gelation in a closed container. A purple gel (MOG-Rh-**1d**) was obtained after *ca* 50 h. After gelation, the wet gel was aged for *ca* 5 h at 85°C . Subsequently, the wet gel was subjected to solvent exchange with ethanol for 3 days. The as-prepared gel was placed into a high pressure Soxhlet extractor (0.75 L). The solvent in the wet gel was extracted with liquid CO_2 (*ca.* 270 g) for 24 h and the extraction temperature was kept at *ca* 19°C . An aerogel (MOA-Rh-**1d**) was obtained after the stainless-steel autoclave was depressurized slowly at RT for about 2-3 h.

For further applications such as gas/dye adsorption and catalysis, the as-synthesized aerogels MOA-Rh-**1a-d** were typically degassed at 85°C for 16 h to remove the solvent molecules. The resulting aerogels are referred to activated aerogels of MOA-Rh-**1a-d**.

2.2 Characterization

N_2 adsorption-desorption isotherms were measured at 77 K with a Quantachrome Autosorb-iQ analyzer. The Brunauer-Emmett-Teller (BET) method was utilized to calculate the specific surface areas. By using the Barrett-Joyner-Halenda (BJH) model, the volume and size distribution of the mesopores were derived from the adsorption branches of isotherms. The volume and size distribution of the micropores were calculated by the Horvath-Kawazoe (HK) theory. Scanning electron micrographs were recorded on a JSM-6330F field emission scanning electron microscope combined with EDS. The samples were prepared by dispersing the aerogel in ethanol and placing on top of conductive glass stubs, and drying at RT followed by drying in vacuum. Prior to examination, the aerogel was coated with a thin layer of gold. Transmission electron micrographs were recorded on a JEOL JEM-2010HR microscope. The samples for TEM were prepared by dispersing the aerogel in ethanol with sonication, and carbon-coated copper grids were placed in the samples three times. Thermogravimetric (TG) analyses were performed under an N_2 atmosphere at a heating rate of $10^\circ\text{C min}^{-1}$ by using a NETZSCH TG 209 system. PXRD patterns were recorded on SmartLab X-ray powder diffractometer (Rigaku Co.) at 40 kV and 30 mA with a Cu target tube. X-ray photoelectron spectroscopy (XPS) was performed on a ULVAC PHI Quantera microprobe. Binding energies (BE) were calibrated by setting the measured BE of C 1s to 284.65 eV. UV-vis spectra were tested on a Shimadzu/UV-3600 spectrophotometer. The X-ray absorption fine structure (XAFS) spectra at Rh K-edge ($E_0 = 23220$ eV) were performed at BL14W1 beam line of Shanghai Synchrotron Radiation Facility (SSRF) operated at 3.5 GeV under "top-up" mode with a constant current of 240 mA.

2.3 Elemental Analysis of the Aerogel

The aerogel MOA-Rh-**1d** (6 mg) was treated with nitric acid (2 mL) and hydrochloric acid (6 mL). The whole mixture was allowed to stay at room temperature for 0.5 h before slowly heated at 200°C until the total volume was reduced to about 0.5 mL. Subsequently, nitric acid (6 mL) and aqueous hydrogen dioxide (30 wt%, 2 mL) were added. The reaction mixture stayed at room temperature for 0.5 h before slowly heated at 200°C until the total volume was reduced to about 0.5 mL. Afterward, nitric acid (6 mL) and HClO_4 (2 mL) were added. The reaction mixture stayed at room temperature for 0.5 h before slowly heated at 200°C until the total volume was reduced to about 0.5 mL. The digestion procedure was repeated ten times. The resulted solution was diluted volumetrically with an aqueous solution of nitric acid (2%) to 100 mL, which was then evaluated by inductively coupled plasma optical emission spectrometer (ICP-OES) for Rh contents. The Rh contents were measured in ppm based on calibration curves obtained with a

series of calibration standard solutions doped with different amount of Rh. The measured Rh content of MOA-Rh-1d was 10.738 ppm (1.0738 mg), and the found Rh% should be 17.9%, using the calculation equation "100% × (1.0738 mg / 6 mg)".

2.4 Dye Adsorption

The dye adsorption studies were carried out by agitating the aerogel MOA-Rh-1d (4.8 mg) in 8 mL of dye solution (20 mg L⁻¹). The dyes of methylene blue (MB) and Coomassie brilliant blue R-250 (BBR-250) were dissolved in water and ethanol, respectively. After adsorption, the dye concentration was determined by UV-vis spectroscopy. The wavenumbers for the UV-vis adsorption for MB and BBR-250 are 664 and 588 nm, respectively.

2.5 Typical Procedure for the Coupling Reactions of CO₂ and Epoxides

A mixture of styrene oxide (**2a**, 240.0 mg, 2 mmol), tetrabutylammonium bromide (NBu₄Br, 8.5 mg, 0.03 mmol) and the activated aerogel MOA-Rh-1d (6.0 mg, 0.005 mmol) was stirring at 100°C under atmospheric CO₂. After 12 h, the reaction mixture was cooled to room temperature. The undissolved catalyst was removed through centrifugation, and washed with ethyl acetate (4 mL × 4). In recycling study, the recovered catalyst was dried under vacuum at room temperature for 6 h and reused in the consecutive run. The combined supernatant was evaporated to dryness. The yield (98%) of 4-phenyl-1,3-dioxolan-2-one (**3a**) was determined by the NMR spectrum of the reaction mixture. ¹H NMR (400 MHz, CDCl₃) of **3a**: δ 7.40 (m, 3H), 7.36 (m, 2H), 5.68 (t, 1H, *J* = 8.0 Hz), 4.79 (m, 1H), 4.30 (m, 1H).

2.6 Typical Procedure for the Catalytic C-H Bond Amination Reactions

A mixture of (*Z*)-methyl 2-azido-3-phenylacrylate (**4a**, 20.3 mg, 0.1 mmol) and the activated aerogel MOA-Rh-1d (4.8 mg, 0.004 mmol) in toluene (0.5 mL) was heated to 80°C. After 16 h, the reaction mixture was cooled to room temperature. The undissolved catalyst was removed through centrifugation, and washed with ethyl acetate (4 mL × 4). In recycling study, the recovered catalyst was dried under vacuum at 100°C for 24 h and reused in the consecutive run. The combined supernatant was evaporated to dryness. The yield (79%) of methyl 1*H*-indole-2-carboxylate (**5a**) was determined by using the NMR spectrum of the reaction mixture. ¹H NMR (400 MHz, CDCl₃) of **5a**: δ 8.98 (br, 1H), 7.68 (d, 1H, *J* = 8.0 Hz), 7.41 (d, 1H, *J* = 8.0 Hz), 7.30 (m, 1H), 7.21 (m, 1H), 7.14 (m, 1H), 3.93 (s, 3H).

2.7 Hot Filtration Experiment

Two parallel C-H amination reactions of **4a** (20.3 mg, 0.1 mmol) in the presence of the activated aerogel MOA-Rh-1d (4.8 mg, 0.004 mmol) were heated in toluene (1 mL) at 80°C. After 6 h, a group of reaction mixture was filtrated by using a 0.45 μm membrane, and the filtrate was allowed to stand at 80°C for another 6 h. The other group of reaction mixture stayed with the catalyst for further reaction without any treatment. The conversion was determined by the NMR spectrum of the reaction mixture.

3. Results and discussion

3.1 Design of MOGs with Rh²⁺-Rh²⁺ Bonds

Although tetracarboxylate Rh₂⁴⁺ dimers are stable under many conditions like strong acids, they participate freely in ligand exchange reactions. As a result, complex dirhodium carboxylate catalysts can be prepared from the exchange reactions of the simplest Rh²⁺ salts, Rh₂(OAc)₄, and carboxylic acids. To develop a MOG with Rh²⁺-Rh²⁺ bonds, a semi-rigid tris-amide-tris-carboxylic ligand H₃btctb was chosen (Scheme 1). Tridentate carboxylate ligands have exhibited great potential for the generation of MOGs, which thus offers possibilities for the development of stable porous MOGs. Most of these works used 1,3,5-benzenetricarboxylic acid (H₃btc) and benzene-1,3,5-trisbenzoic acid (H₃btb) as ligands and M³⁺ (e.g. Fe³⁺, Cr³⁺, Co³⁺) salts as the metal sources.²⁵⁻²⁹ The amide groups in H₃btctb have dual functions. On one hand, the amide groups increase the size of the trigonal ligand, which could potentially generate a large inner cavity in a MOG. On the other hand, the amide can serve as versatile hydrogen-bonding donor and acceptor groups, often used as the driving force for gelation. Recently, Schmidt and Albuquerque et al. and Dastidar et al. independently have developed luminescent Cd^{II}-MOGs derived from the ligand H₃btctb.^{30,31}

MOFs based on H₃btctb with definite crystal structures have been reported by several groups.³²⁻³⁴ Lah et al. prepared a MOF with the formula of Cu₃(btctb)₂(H₂O)₂ with a (3,4)-connected **pto** net topology, where the ligand btctb³⁻ served as a 3-connected node and the Cu₂(CO₂)₄ paddle-wheel building units acted as a planar 4-connected node.³² It is noted that the reaction of Cu²⁺ ion and H₃btc, a rigid tricarboxylic acid, has led to the formation of a MOF of (3,4)-connected **tbo** net topology with dicopper units, Cu₃(btc)₂ (HKUST-1).³⁵ Considering that Rh₂(CO₂)₄ and Cu₂(CO₂)₄ have the similar dinuclear paddle-wheel structures, comparable (3,4)-connected coordination polymeric networks are hypothesized to be formed from the reaction of Rh₂(OAc)₄ and H₃btctb (Figure 1). However, it should be noticed that the gel network is definitely different from the long-range ordered (3,4)-connected MOFs based on H₃btctb ligand because the metal-ligand linking during gelation is expected to extend irregularly and non-continuously in all dimensions.

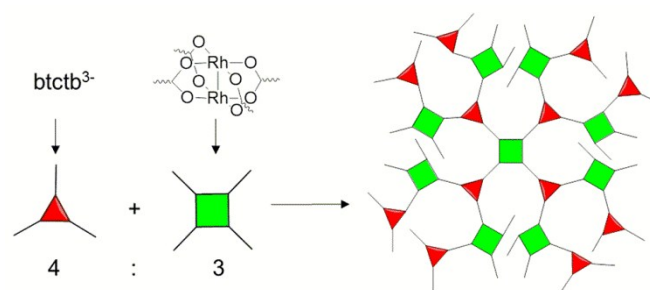


Figure 1. Schematic representation of the plausible coordination polymeric network with Rh²⁺-Rh²⁺ bonds.

3.2 Gelation Study

The reaction between $\text{Rh}_2(\text{OAc})_4$ and H_3btctb (0.0075 mol/L) in a 3:4 molar ratio in DMF/ H_2O (20:1 v/v) at 85°C gave a yellow gel (MOG-Rh-1a) after 50 h (Table S1, entry 1). It was found that the elevated temperature was a requisite for gelation, while a similar reaction at RT didn't give rise to a gel. The gelation state was evaluated by turning the vial upside down. While keeping the 3:4 molar ratio of $\text{Rh}_2(\text{OAc})_4$ and H_3btctb , the molar concentration range for H_3btctb (C_L) between 0.0075 to 0.0225 mol/L was found to be optimal for the gel formation in DMF/ H_2O (20:1 v/v). The colors of the gels (MOG-Rh-1a, $C_L = 0.0075$ mol/L; MOG-Rh-1b, $C_L = 0.015$ mol/L; MOG-Rh-1c, $C_L = 0.0225$ mol/L) darkened with the increase of the concentration (Figure 2; Table S1, entries 1-3).



Figure 2. Representative photographic images of gels (from left to right: MOG-Rh-1a, -1b, -1c and -1d).

The tricarboxylic acid H_3btctb has a good solubility in DMF, but isn't dissolved in other common solvents such as alcohol, acetone and chloroform, so mixing solvent systems were explored in gelation tests. Water is necessary for gelation, and a series of control experiments disclosed that no gelation could occur when the content of water was under 5% by volume in the DMF/ H_2O (Table S2, entries 1-4). Gels could be also produced from the DMF/alcohol mixtures by heating (entries 5-8). The minimum volume percentages of methanol and ethanol in the mixed DMF/alcohol solvent are 5% and 25%, respectively. The necessity of water or alcohols suggested that hydrogen bonding should be involved in the gel formation, since the coordination network contains a plenty of amide groups.

Moreover, a series of studies were carried out to determine the influence of the counteranion on the gelation phenomenon. Interestingly, the use of other dirhodium carboxylates such as dirhodium pivalate ($\text{Rh}_2(\text{Piv})_4$) and dirhodium trifluoroacetate ($\text{Rh}_2(\text{TFA})_4$) in 1:1 DMF/MeOH led to the formation of an orange red gel and a dark green gel, respectively (Table S3). In comparison, the reaction between H_3btctb and $\text{Rh}_2(\text{OAc})_4$ in 1:1 DMF/MeOH gave rise to a purple gel (MOG-Rh-1d, Figure 2). Trials using $[\text{Rh}^{\text{I}}\text{Cl}(\text{COD})_2]$ and $\text{Rh}^{\text{III}}\text{Cl}_3$ for gelation failed (Table S4), indicative of the importance of dirhodium(II) units for the gelation formation.

We selected two tricarboxylic acids 1,3,5-tri(4-carboxyphenoxy)benzene (H_3tcpb) and 4,4',4''-[benzene-1,3,5-triyltris(azanediyl)]tribenzoic acid (H_3tatab) in addition to H_3btctb to

study the influences of the nature of the ligands on the gelation results. Instead of amide groups in H_3btctb , ethers and amines are incorporated in H_3tcpb and H_3tatab , respectively (Table S5). Besides, H_3tatab possesses a triazine ring. It is noted that the triazine-based plane can serve as a potential π - π stacking center. The π - π stacking is usually an important aromatic nitrogen heterocycles. Under similar conditions as H_3btctb , the gelation experiments with H_3tcpb or H_3tatab were carried out. It was found that no gels but precipitates were formed. For the discussion convenience, the formed precipitated from the reactions with H_3tcpb and H_3tatab are named as Rh-tcpb and Rh-tatab, respectively. The results might suggest that hydrogen bonding played an important role in gel formation, whereas π - π stacking was not a determining factor.

The gels of MOG-Rh-1a-d are non-thermoreversible, indicative of the coordination polymeric nature of the gel network. When the gels were heated up to 100°C, neither their appearance changed nor any solvent has leaked from the gel, whereas they suffered fragmentation if they were heated at a higher temperature (e.g. 120°C, Figure S1).

The gels of MOG-Rh-1a-d are stable at the bench for at least 3 months. The gels are also stable when immersed in common solvents (e.g. alcohol, acetone, toluene, CHCl_3 , DMSO, DMF and DME) for at least one week. Further stability tests disclosed that no fragmentation occurred after the gels were immersed in boiled water for 3 h, but the color turned from purple to green (Figure S2). It might be explained that most of the coordinated DMF molecules have been replaced by water. On the basis of the study of Johnson et al. and Jessop et al. on the coordination effects of solvents, dirhodium(II) complexes with oxygen-containing solvents (e.g. H_2O , THF) in the axial position were usually in green, whereas those with nitrogen-containing solvents (e.g. DMF, MeCN, NEt_3) were often in purple.^{36,37}

We also checked the pH range in which MOG-Rh-1a-d can resist. After immersing in aqueous solutions with the pH range of 1-10 for 6 h, the bulk gels were found to be stable (Figure S3). Nevertheless, concentrated HCl (12 M) caused precipitation, indicating that the networks of MOG-Rh-1a-d have been disrupted (Figure S4).

The thixotropic nature of MOG-Rh-1a-d was examined by shaking the gel for 10 min, which turned the gels into liquid (Figure S5).³⁸ However, after standing at RT for 7 days, the liquid could not reform a gel, indicating that the networks of MOG-Rh-1a-d has decomposed.

3.3 Preparation and Characterizations of Aerogels

To remove the excess amount of starting materials, the gels MOG-Rh-1a-d were subjected to solvent exchange with ethanol for 3 days. The resulting purified gels were placed into a high pressure Soxhlet extractor, and the adsorbed ethanol molecules were exchanged with CO_2 for 24 h to produce green metal-organic aerogels MOA-Rh-1a-d (Figure S6). The aerogels MOA-Rh-1a-d are insoluble in common organic solvents, such as toluene, DMSO, DMF, acetone and acetonitrile. We have

therefore carried out a series of physical characterization experiments in order to test its solid properties.

Scanning electron microscopy (SEM) and transmission electron microscopy (TEM) were used to check the morphology and microstructures of the aerogels of MOA-Rh-**1b**, -**1c** and -**1d** as representatives, which were prepared from MOG-Rh-**1b**, -**1c** and -**1d**, respectively (Figure 3). The SEM images reveal that they all possess spongy porous microstructures, which are made up of spherical interconnected particles with relatively uniform size of *ca* 50 nm (Figure 3a-c). The TEM images again disclose the aerogels are of pore structures of *ca* 10-20 nm in diameter (Figure 3d-f).

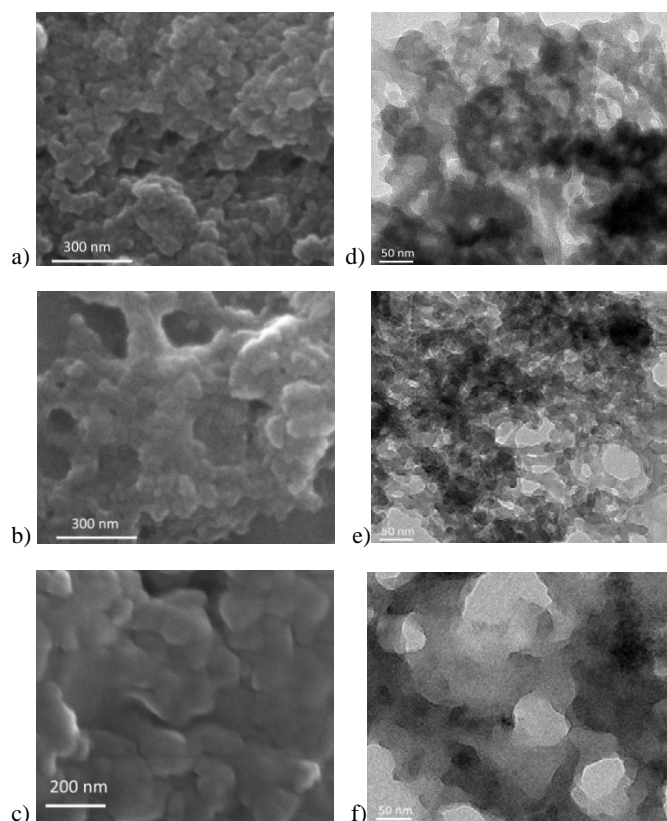


Figure 3. SEM and TEM images of the aerogels MOA-Rh-**1b** (a,d), MOA-Rh-**1c** (b,e) and MOA-Rh-**1d** (c,f).

The aerogels (MOA-Rh-**1b-d**) were subjected to energy-dispersive X-ray spectroscopy (EDS) analysis, disclosing the presence of C, O and Rh elements (Figure S7). ICP spectrometric evaluation discloses that the Rh content of MOA-Rh-**1d** is 17.9%, whereas the calculated Rh% (based on the theory formula of $(\text{Rh}_2)_3(\text{btctb})_4$) is 21.5%. The lower Rh content might be due to the incomplete deprotonation of the carboxylic groups of H_3btctb .

Thermogravimetric analysis (TGA) of the aerogel MOA-Rh-**1d** shows a total weight loss of 19% in the range of 24-298°C, corresponding to the loss of the solvents absorbed on the particle surface and in the pores (Figure S8). The coordination network might collapse above 298°C. TG analyses of MOA-Rh-**1b** and MOA-Rh-**1c** show similar curves to that of MOA-Rh-**1d**,

indicating that the coordination networks might collapse above 311°C for the two aerogels.

The aerogels are amorphous according to the powder XRD patterns, which exhibit only weak and broad peaks (Figure S9). The surface analyses of aerogels were done by the X-ray photoelectron spectroscopy (XPS). The XPS spectra display two intense peaks at 314.0 ± 0.2 and 309.2 ± 0.1 eV assigned to Rh $3d_{3/2}$ and Rh $3d_{5/2}$, respectively, indicative of the +2 valence nature of Rh (Figure S10). According to the literatures, the $3d_{5/2}$ binding energy of oxidized Rh^{2+} is in the range of 308.4 and 309.3 eV.³⁹ The solid UV-vis spectra of aerogels MOA-Rh-**1b-d** display a broad band around 580-600 nm (Figure S11). These bands are characteristic of the dirhodium paddle-wheel structure, which are assigned to the HOMO-LUMO ($\pi^*(\text{Rh}_2) \rightarrow \sigma^*(\text{Rh}_2)$) transition.⁴⁰ The presence of the dirhodium paddle-wheel units are further confirmed by the X-ray absorption spectroscopy (XAS).¹⁸ Based on the XAS data of MOA-Rh-**1d** (Figure S12, Table S6), the average Rh-O and Rh-Rh bonds in MOA-Rh-**1d** are calculated to be 2.04 and 2.40 Å, respectively.

3.4 Gas Adsorption and Pore Analyses

To evaluate the porosity of the aerogels MOA-Rh-**1a-d**, the adsorption isotherms of N_2 at 77 K have been studied (Figure 4). The aerogels generally show type-IV adsorption behaviors with clear hysteresis loops in the nitrogen isotherms. Observation of abrupt adsorption at low pressure indicates that both micro- and meso-porosity are present. The gas sorption parameters of the aerogels MOA-Rh-**1a-d** are shown in Table 1.

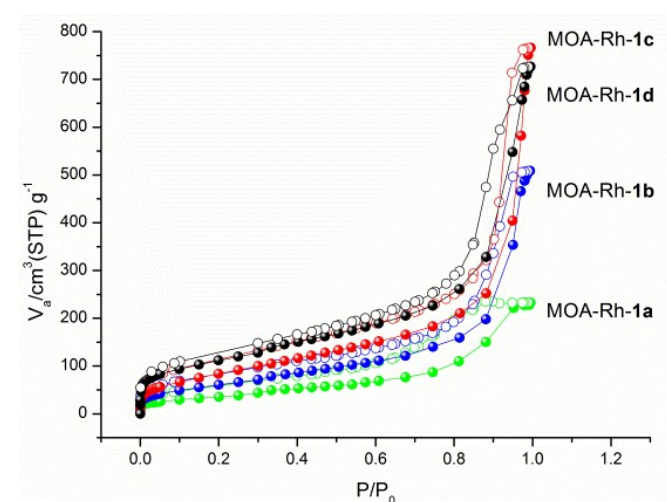


Figure 4. Nitrogen adsorption-desorption isotherms of the aerogels MOA-Rh-**1a-d** at 77 K.

The specific surface areas and porosities are found to depend on the precursor concentration used for the gel formation. The ligand concentrations (C_l) of MOA-Rh-**1a**, -**1b**, and -**1c** are 0.075, 0.015 and 0.0225 mol/L, respectively. Based on the N_2 adsorption isotherm at 77 K, the Brunauer-Emmett-Teller (BET) surface areas of MOA-Rh-**1a**, -**1b**, and -**1c** are 131,

Table 1. Porosity Properties of Representative Aerogels.

Aerogels ^a	S_{BET} ($\text{m}^2 \text{g}^{-1}$) ^b	S_{micro} ($\text{m}^2 \text{g}^{-1}$) ^c	V_t ($\text{cm}^3 \text{g}^{-1}$) ^d	V_{meso} ($\text{cm}^3 \text{g}^{-1}$) ^e	V_{micro} ($\text{cm}^3 \text{g}^{-1}$) ^f	$D_{\text{meso}}^g/D_{\text{micro}}^h$ (nm)
MOA-Rh-1a	131	25	0.36	0.34	0.04	7.8/0.9
MOA-Rh-1b	230	9	0.79	0.72	0.06	14.1/1.1
MOA-Rh-1c	323	-	1.19	1.08	0.07	13.9/1.1
MOA-Rh-1d	405	84	1.12	1.03	0.11	15.9/1.1

^aThe aerogels MOA-Rh-1a-d were obtained from the corresponding gels MOG-Rh-1a-d with preparation details as shown in Experimental Section. Galation temperature and degassing temperature are both 85°C. ^b S_{BET} is the BET-specific surface area. ^c S_{micro} is the t-plot-specific micropore surface area. ^d V_t is the total specific pore volume. ^e V_{meso} is the specific mesopore volume calculated from adsorption isotherm using the BJH method. ^f V_{micro} is the specific micropore volume calculated using the SF method. ^g D_{meso} is the mesopore diameter calculated from adsorption isotherm using the BJH method. ^h D_{micro} is the micropore diameter calculated from adsorption isotherm using the SF method.

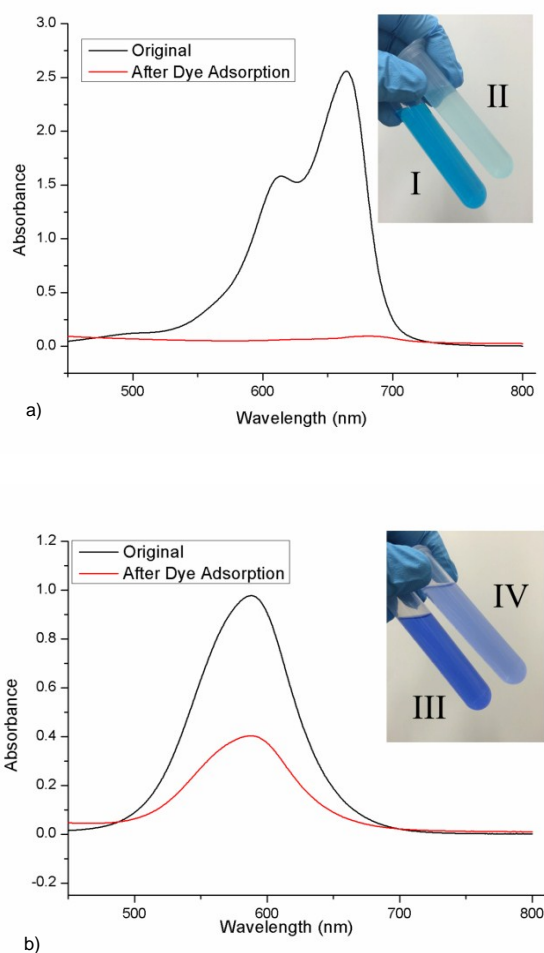


Figure 5. The UV-vis spectra for the dye uptake experiments of MB (a) and BBR-250 (b) for MOA-Rh-1d. The inserts show picture of the dye-polluted solvents before (I, III) and after (II, IV) dye adsorption.

230 and 323 $\text{m}^2 \text{g}^{-1}$, respectively, indicating that the surface area increased with the concentration of H_3btctb used for gelation. The Barrett-Joyner-Halenda (BJH) mesoporous volumes of MOA-Rh-1a, -1b, and -1c increase from 0.34 to 1.08 $\text{cm}^3 \text{g}^{-1}$, and their Saito-Foley (SF) microporous volumes also increase from 0.04 to 0.07 $\text{cm}^3 \text{g}^{-1}$. The BJH mesoporous size of MOA-Rh-1c is centered around 14 nm, whereas those of MOA-Rh-1a and -1b display a much wider distribution (Figure S13).

The specific surface areas and porosities could be further tuned by the solvents used in gelation. MOA-Rh-1b and MOA-Rh-1d were prepared with the same concentration ($C_L = 0.015$ mol/L), but in different solvents (e.g. 20:1 v/v DMF/ H_2O for the former and 1:1 v/v DMF/MeOH for the latter). The BET surface area of MOA-Rh-1d (405 $\text{m}^2 \text{g}^{-1}$) was much larger than that of MOA-Rh-1b (230 $\text{m}^2 \text{g}^{-1}$). The BJH mesoporous sizes of MOA-Rh-1b and -1d are 14 and 16 nm, respectively.

3.5 Uptake of Bulky Molecules from Solution

To verify the accessibility of the aerogels for bulky molecule insertion, the aerogel MOA-Rh-1d was selected as a representative for the dye uptake test. The adsorption of methylene blue (MB, $14.4 \times 6.1 \text{ \AA}^2$) and Coomassie brilliant blue R-250 (BBR-250, $22 \times 18 \text{ \AA}^2$) was studied by UV-vis spectroscopy. MOA-Rh-1d is found to be efficient in the adsorption of the dyes. After 24 h, 96% of MB (32 mg g^{-1} , the adsorption amount of the dye per gram of the aerogel) or 59% of BBR-250 (19.7 mg g^{-1}) was adsorbed on the aerogel (Figure 5). The capability to host a dye molecule with the approximate dimension of $2.2 \times 1.8 \text{ nm}^2$ (BBR-250) suggested that MOA-Rh-1d may have an ability to up-take large substrates and product molecules in catalytic reactions.

3.6 Catalytic Performances of Aerogels

Considering that the aerogels MOA-Rh-1a-d aren't dissolved in common organic solvents, we have tested their heterogeneous catalysis. Heterogenization of a dirhodium(II) catalyst has ever been achieved by ligand exchange with a solid-supported acid, axial coordination to polymer-supported pyridine, or copolymerization of Rh(II)-complex-containing monomer.⁴¹⁻⁴⁴

Heterogeneous catalysts of dirhodium(II)-containing MOFs and MOCs have also been developed.^{10,16,18,19} It is generally acknowledged that the porous materials which possess higher surface areas should display better catalysis behaviors.⁴⁵ Among all of the MOAs, MOA-Rh-1d possesses the largest BET surface area, and then is used for catalysis study.

Organic transformations using CO₂ as cheap C1 sources have attracted a lot of interests. One of the most important reactions is the coupling reaction of CO₂ and epoxides to produce cyclic carbonates, which can be found in a wide range of industrial applications, including as polar solvents, precursors for polycarbonate materials, and electrolytes in lithium secondary batteries.⁴⁶

Table 2. Cycloaddition of CO₂ and epoxides.^a

Entry	Catalyst	Epoxide	Yield (%)
1	MOA-Rh-1d	2a	98%
2	Rh ₂ (OAc) ₄	2a	67%
3	Rh-tcpb	2a	76%
4	Rh-tatab	2a	61%
5	No metal catalyst	2a	44%
6	MOA-Rh-1d	2b	98%
7	MOA-Rh-1d	2c	99%

^aReaction condition: catalyst (0.005 mmol, 0.25 mol%), NBu₄Br (8.5 mg, 0.03 mmol, 1.5 mol%) and epoxide (2 mmol, 1 eq).

To test the catalytic capability of our metal-organic aerogel catalyst in the valuable reactions relating to CO₂ utilization, a model reaction of the coupling reaction of CO₂ and styrene oxide (**2a**) was carried out. In the presence of MOA-Rh-1d (0.25 mol%) and the co-catalyst NBu₄Br (1.5 mol%), cycloaddition of CO₂ (excess) to **2a** under the atmospheric pressure led to the formation of cyclic carbonate **3a** in 98% yield (Table 2, entry 1). Under the similar condition, the reactions in the presence of Rh₂(OAc)₄, Rh-tcpb and Rh-tatab gave rise to **3a** in 67%, 76% and 61% yields, respectively (entries 2-4). In comparison, **3a** was produced in only 44% yield in the presence of NBu₄Br but without the addition of

metal catalyst (entry 5). These results indicate that gel formation is crucial to exhibit better catalytic activities. In addition to styrene oxide, other epoxides such as 2-(butoxymethyl)oxirane (**2b**) and 2-(phenoxymethyl)oxirane (**2c**) can react with an excess amount of CO₂ under the atmospheric pressure to produce the cyclic carbonates **3b** and **3c** in almost 100% yield (entries 6 and 7).

To verify the reaction was heterogeneous but not catalyzed by the dissociated Rh species that were leached into the reaction solution, we have carried out inductively coupled plasma optical emission spectrometer (ICP-OES) analysis of the reaction filtrate with the removal of the MOA-Rh-1d after the catalytic reaction was done, which indicated that the amount of the rhodium leaching into the reaction mixture was 0.8% of the total Rh content in MOA-Rh-1d. Pleasantly, the aerogel MOA-Rh-1d catalyst can be easily isolated by centrifugation and reused at least ten times, and the yields were in the range of 91-98% for the ten successive runs (Figure 6, Table S7a). The presence of dinuclear rhodium paddle-wheel units and the Rh²⁺ valence in the recycled MOA-Rh-1 after catalysis are proven by UV-vis and XPS spectra, respectively. The XPS spectrum of the recycled MOA-Rh-1d sample displays two intense peaks at 313.8 and 309.2 eV assigned to Rh 3d_{3/2} and Rh 3d_{5/2}, respectively, suggesting that the Rh²⁺ metal sites haven't been oxidized to higher states such as Rh³⁺ (Figure S10d). Furthermore, the solid UV-vis spectrum of MOA-Rh-1d after catalysis exhibits a broad band around 592 nm, which is only 8 nm blue shift away from the as-synthesized MOA-Rh-1d sample (Figure S11b). The existence of the characteristic π*(Rh₂)→σ*(Rh₂) transition adsorption peak indicative of the dirhodium paddle-wheel structure in the recycled catalyst.⁴⁰

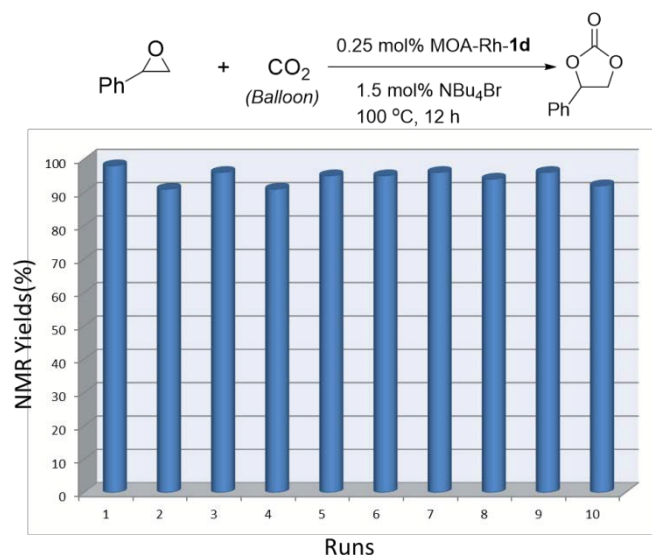
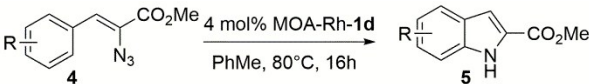


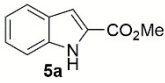
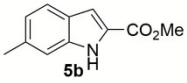
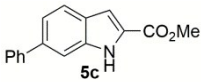
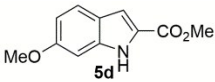
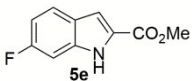
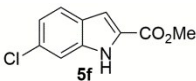
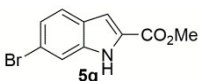
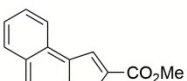
Figure 6. Recycling experiments.

C-H Amination has been greatly enhanced due to the improved methods of the syntheses of rhodium nitrene intermediates.²⁰ As test reactions, C-H amination of vinyl azides were chosen.^{19,47} The evaluation of the gel catalyst was

initially carried out using the intramolecular C-H amination of (*Z*)-methyl 2-azido-3-phenylacrylate (**4a**) in the presence of MOA-Rh-**1d** (4 mol%) in toluene at 80 °C as the standard reaction. After 12 h, methyl 1*H*-indole-2-carboxylate (**5a**) was produced in 47% yield (Table S8, entry 1). The modest conversion might be explained that not all of the coordinated DMF solvent molecules on the Rh²⁺ centers of the aerogel MOA-Rh-**1d** have been removed. For better treatment, the aerogel MOA-Rh-**1d** was subjected to further solvent exchange with dimethoxyethane (DME) for 3 days and activated by heating at 110 °C under vacuum for 24 h. The activated DME-exchanged MOA-Rh-**1d** displays a much better performance, promoting the reaction with **4a** to generate **5a** with 79% conversion after 12 h (entry 2). For comparison, under the similar reaction conditions, the reactions in the presence of 4 mol% of Rh₂(OAc)₄, Rh-tcpb and Rh-tatab led to the formation of **5a** in the yields of 18%, 26% and 54% (entries 3-5). The results again suggest that our aerogel catalysts exhibit superior activities.

Table 3. Substrate Scope of Catalytic C-H Amination.^a



Entry	Product	Entry	Product
1	 79%	2	 92%
3	 74%	4	 91%
5	 86%	6	 88%
7	 81%	8	 100%

^aProvided are the conversions of vinyl azides to indoles.

To explore the substrate scope of the aerogel MOA-Rh-**1d**-catalyzed reactions, a range of vinyl azides have been studied (Table 3). In the presence of a catalytic amount of MOA-Rh-**1d**, the reactions with *para*-methyl and *para*-phenyl azidoacrylates gave indole products **5b** and **5c**, respectively, with high conversions (entries 2 and 3). Vinyl azides with electron-

donating and electron-withdrawing aryl substituents have also employed in the catalysis, and indole products with good to excellent yields can be generated (entries 3-7). In addition to indoles, aromatic *N*-heterocycles such as **5h** can be accessed from 1-substituted naphthalene vinyl azide (entry 8).

To confirm the heterogeneity of the reaction, we have carried out a hot filtration experiment (Figure 7). At the 47% conversion of the intramolecular C-H amination reaction with **4a** in the presence of MOA-Rh-**1d** for 6 h, the reaction mixture was filtrated with filtration membrane (0.45 μm), and the filtrate was heating at 80°C for another 6 h. The conversion of the supernatant didn't increase and remained to be 47%. In contrast, a parallel reaction with the catalyst reached around 79% conversion after heating at 80°C for the same reaction time. ICP-OES analysis of the reaction filtrate indicated that the amount of the rhodium leaching into the reaction mixture was 0.6% of the total Rh content in MOA-Rh-**1d**. The aerogel MOA-Rh-**1d** catalyst can be reused for three times without significant loss of activity (Table S7b).

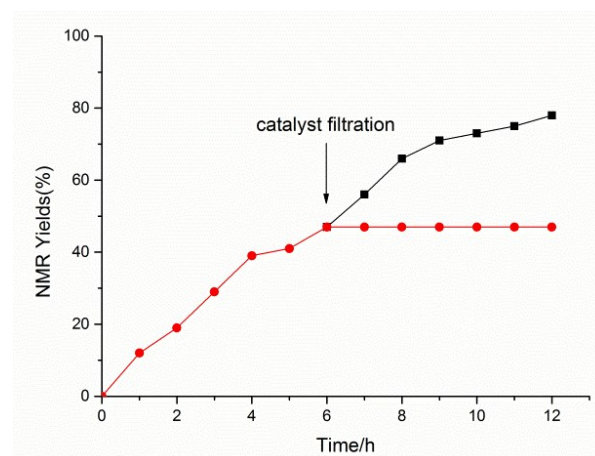


Figure 7. Filtration experiment for aerogel MOA-Rh-**1d**. Conversions are given as a function of time. The full square (■) represents the reaction with aerogel MOA-Rh-**1d** as a catalyst. The full cycle (●) represents the reaction after removal of aerogel MOA-Rh-**1d** at (47%) conversion.

Conclusions

A functional micro/mesoporous metal-organic aerogel (MOA-Rh-**1d**) with Rh²⁺-Rh²⁺ bonds, which can efficiently promote cycloaddition of CO₂ and epoxides as well as intramolecular C-H amination of vinyl azides, has been prepared from the corresponding metal-organic gel (MOG-Rh-**1d**), whereas the latter was produced from the reaction of Rh₂(OAc)₄ and the tricarboxylic acid 4,4',4''-[1,3,5-benzenetriyltris(carbonylimino)] trisbenzoic acid (H₃btctb) in 1:1 DMF/methanol. Gelation study disclosed that coordination and hydrogen-bonding were responsible for the gel formation. Further study on the design, synthesis and catalytic applications of more aerogel catalysts based on dirhodium(II) units are in the progress.

Acknowledgements

This work was supported by the 973 Program (2012CB821701) and the NSFC Projects (21373278, 91222201 and 21450110063), the STP Project of Guangzhou (15020016), the NSF of Guangdong Province (S2013030013474) and the RFDP of Higher Education of China (20120171130006).

References

- M.-O. M. Piepenbrock, G. O. Lloyd, N. Clarke, J. W. Steed, *Chem. Rev.*, 2010, **110**, 1960-2004.
- J. Y. Zhang, C.-Y. Su, *Coord. Chem. Rev.*, 2013, **257**, 1373-1408.
- A. Y. Y. Tam, V. W. W. Yam, *Chem. Soc. Rev.*, 2013, **42**, 1540-1567.
- J. Y. Zhang, X. Wang, L. He, L. P. Chen, C.-Y. Su, S. L. James, *New J. Chem.*, 2009, **33**, 1070-1075.
- J. Huang, L. He, J. Y. Zhang, L. P. Chen, C.-Y. Su, *J. Mol. Catal. A: Chem.*, 2010, **317**, 97-103.
- A. Kishimura, T. Yamashita, T. Aida, *J. Am. Chem. Soc.*, 2005, **127**, 179-183.
- F. Camerel, R. Ziessel, B. Donnio, C. Bourgogne, D. Guillon, M. Schmutz, C. Iacovita, J.-P. Bucher, *Angew. Chem., Int. Ed.*, 2007, **46**, 2659-2662.
- F. A. Cotton, C. Lin, C. A. Murillo, *J. Am. Chem. Soc.*, 2001, **123**, 2670-2671.
- P. Angaridis, J. F. Berry, F. A. Cotton, C. A. Murillo, X. Wang, *J. Am. Chem. Soc.*, 2003, **125**, 10327-10334.
- F. A. Cotton, C. A. Murillo, S.-E. Stiriba, X. Wang, R. M. Yu, *Inorg. Chem.*, 2005, **44**, 8223-8233.
- F. A. Cotton, E. V. Dikarev, M. A. Petrukhina, M. Schmitz, P. J. Stang, *Inorg. Chem.*, 2002, **41**, 2903-2908.
- J.-R. Li, A. A. Yakovenko, W. Lu, D. J. Timmons, W. Zhuang, D. Q. Yuan, H.-C. Zhou, *J. Am. Chem. Soc.*, 2010, **132**, 17599-17610.
- M. D. Young, Q. Zhang, H.-C. Zhou, *Inorg. Chem. Acta*, 2015, **424**, 216-220.
- W. Mori, T. Sato, T. Ohmura, C. N. Kato, T. Takeji, *J. Solid State Chem.*, 2005, **178**, 2555-2573.
- Y. Kataoka, K. Sato, Y. Miyazaki, K. Masuda, H. Tanaka, S. Naito, W. Mori, *Energy Environ. Sci.*, 2009, **2**, 397-400.
- T. Sato, W. Mori, C. N. Kato, E. Yanaoka, T. Kuribayashi, R. Ohtera, Y. Shiraishi, *J. Catal.*, 2005, **232**, 186-198.
- C. R. Wade, M. Dincă, *Dalton Trans.*, 2012, **41**, 7931-7938.
- G. Nickerl, U. Stoeck, U. Burkhardt, I. Senkowska, S. Kaskel, *J. Mater. Chem. A*, 2014, **2**, 144-148.
- L. Chen, T. Yang, H. Cui, T. Cai, L. Zhang and C.-Y. Su, *J. Mater. Chem. A*, 2015, **3**, 20201-20209.
- J. L. Roizen, M. E. Harvey, J. Du Bois, *Acc. Chem. Res.*, 2012, **45**, 911-922.
- X. Song, Y. Zou, X. Liu, M. Oh, M. S. Lah, *New J. Chem.*, 2010, **34**, 2396-2399.
- K. Matsumoto, T. Higashihara, M. Ueda, *Macromolecules*, 2008, **41**, 7560-7565.
- Q.-R. Fang, D.-Q. Yuan, J. Sculley, J.-R. Li, Z.-B. Han, H.-C. Zhou, *Inorg. Chem.*, 2010, **49**, 11637-11642.
- W. G. Shou, J. Li, T. Guo, Z. Lin, G. Jia, *Organometallics*, 2009, **28**, 6847-6854.
- Q. Wei, J. S. L. James, *Chem. Commun.*, 2005, 1555-1556.
- J. Yin, G. Yang, H. Wang, Y. Chen, *Chem. Commun.*, 2007, 4614-4616.
- M. R. Lohe, M. Rose, S. Kaskel, *Chem. Commun.*, 2009, 6056-6058.
- S. K. Nune, P. K. Thallapally, B. P. McGrail, *J. Mater. Chem.*, 2010, **20**, 7623-7625.
- S. Xiang, L. Li, J. Y. Zhang, X. Tan, H. Cui, J. Shi, Y. Hu, L. P. Chen, C.-Y. Su, S. L. James, *J. Mater. Chem.*, 2012, **22**, 1862-1867.
- A. Bernet, R. Q. Albuquerque, M. Behr, S. T. Hoffmann, H.-W. Schmidt, *Soft. Matter.*, 2012, **8**, 66-69.
- S. Banerjee, N. N. Adarsh, P. Dastidar, *Soft. Matter.*, 2012, **8**, 7623-7629.
- L. Rajput, D. Kim, M. S. Lah, *CrystEngComm*, 2013, **15**, 259-264.
- R. Grönker, V. Bon, P. Müller, U. Stoeck, S. Krause, U. Mueller, I. Senkowska, S. Kaskel, *Chem. Commun.*, 2014, **50**, 3450-3452.
- Y.-Q. Chen, Y.-K. Qu, G.-R. Li, Z.-Z. Zhuang, Z. Chang, T.-L. Hu, J. Xu, X.-H. Bu, *Inorg. Chem.*, 2014, **53**, 8842-8844.
- S. S.-Y. Chui, S. M.-F. Lo, J. P. H. Charmant, A. G. Orpen, I. D. Williams, *Science*, 1999, **283**, 1148-1150.
- S. A. Johnson, H. R. Hunt, H. M. Neumann, *Inorg. Chem.*, 1963, **2**, 960-962.
- D. C. Wynne, M. M. Olmstead, P. G. Jessop, *J. Am. Chem. Soc.*, 2000, **122**, 7638-7647.
- S. Roy, A. K. Katiyar, S. P. Mondal, S. P. Mondal, S. K. Ray, K. Biradha, *ACS Appl. Mater. Interfaces*, 2014, **6**, 11493-11501.
- J. F. Múnera, S. Irusta, L. M. Cornaglia, E. A. Lombardo, D. V. Cesar, M. Schmal, *J. Catal.*, 2007, **245**, 25-34.
- T. P. Zhu, M. Q. Ahsan, T. Malinski, K. M. Kadish, J. L. Bear, *Inorg. Chem.*, 1984, **23**, 2-3.
- M. P. Doyle, M. Yan, H.-M. Gau, E. C. Blossey, *Org. Lett.*, 2003, **5**, 561-563.
- H. M. L. Davies, A. M. Walji, T. Nagashima, *J. Am. Chem. Soc.*, 2004, **126**, 4271-4280.
- K. Takeda, T. Oohara, M. Anada, H. Nambu, S. Hashimoto, *Angew. Chem., Int. Ed.*, 2010, **49**, 6979-6983.
- K. Kaneda, M. Terasawa, T. Imanaka, S. Teranishi, *Chem. Lett.*, 1976, **5**, 995-998.
- J. Liu, L. Chen, H. Cui, J. Zhang, L. Zhang and C. Y. Su, *Chem. Soc. Rev.*, 2014, **43**, 6011-6061.
- M. Aresta, R. van Eldik, *Advances in Inorganic Chemistry*, 2014, volume **66**.
- B. J. Stokes, H. Dong, B. E. Leslie, A. L. Pumphrey, T. G. Driver, *J. Am. Chem. Soc.*, 2007, **129**, 7500-7501.